

The Proper Scan Delay of the Hepatobiliary Phase of Gadoteric Acid-Enhanced Magnetic Resonance Imaging to Evaluate Small-Sized (≤ 3 cm) Hepatocellular Carcinoma in Cirrhotic Liver¹

간경변증 환자에서 소간세포암평가를 위한 Gadoteric Acid 조영증강 자기공명영상의 적절한 스캔지연¹

Ji Hyun Lee, MD², Yong Yeon Jeong, MD¹, Sook Hee Heo, MD¹, Sang Soo Shin, MD², Jin Woong Kim, MD¹, Heung Keun Kang, MD¹

¹Department of Radiology, Chonnam National University Hwasun Hospital, Chonnam National University Medical School, Hwasun, Korea

²Department of Radiology, Chonnam National University Hospital, Chonnam National University Medical School, Gwangju, Korea

Purpose: To assess the optimal scan delay of hepatobiliary phase of gadoteric acid (GA)-enhanced magnetic resonance (MR) imaging for small-sized (≤ 3 cm) hepatocellular carcinomas (HCCs) in cirrhotic liver.

Materials and Methods: There were 71 HCCs included in this study, derived from 53 patients with liver cirrhosis. Hepatobiliary phase MR imaging was obtained at 10, 15 and 20 mins after GA injection. For quantitative analysis, 2 radiologists calculated signal to noise ratio (SNR), enhancement ratio (ER) of the tumor and liver parenchyma and contrast-to-noise ratio (CNR) at 10 min, 15 min, and 20 min images, respectively. For qualitative analysis, 3 radiologists independently reviewed the 3 different phase about HCC possibilities using a 5-point scale. For each observer, the diagnostic accuracy of different hepatobiliary phases was compared using the area under the alternative free-response receiver operating characteristic curve (Az). In addition, sensitivity and specificity were compared.

Results: No significant differences in SNR, ER and CNR at 10 min, 15 min, and 20 min were found. The Az values for HCC possibility were not significantly different. Sensitivity and specificity were also not significantly different.

Conclusion: Hepatobiliary phase MR imaging were obtained at 10 min, 15 min and 20 min yield comparable diagnostic information, so that the choice of scan delay can be adapted according to the clinical routine needs.

Index terms

Hepatocellular Carcinoma
Cirrhosis of Liver
Magnetic Resonance Imaging
Gadolinium Ethoxybenzyl
Diethylenetriamine Pentaacetic Acid

Received December 10, 2012; Accepted February 13, 2013

Corresponding author: Yong Yeon Jeong, MD
Department of Radiology, Chonnam National University
Hwasun Hospital, Chonnam National University Medical
School, 322 Seoyang-ro, Hwasun-eup, Hwasun 519-763,
Korea.
Tel. 82-61-379-7133 Fax. 82-61-379-7101
E-mail: yjeong@jnu.ac.kr

This is an Open Access article distributed under the terms of the Creative Commons Attribution Non-Commercial License (<http://creativecommons.org/licenses/by-nc/3.0>) which permits unrestricted non-commercial use, distribution, and reproduction in any medium, provided the original work is properly cited.

INTRODUCTION

Gadoteric acid (GA) is a liver-specific contrast agent that is used for magnetic resonance (MR) imaging. GA has features of a bolus-injectable extracellular contrast agent and a late hepatocyte-specific phase (1). After intravenous injection, GA is transported from the extracellular space into the hepatocytes and is subsequently excreted into the biliary canaliculi. GA accumulates in normally functioning hepatocytes at the hepatobiliary phase, so the hepatic parenchyma is enhanced (1-5). The use of GA for liver MR imaging has proven to be valuable

in both the detection and characterization of focal hepatic lesions. In particular, the GA-enhanced hepatobiliary phase MR imaging may assist in better diagnosis of hepatocellular carcinoma (HCC) and thus, may help guide in the treatment planning (6-13).

The hepatic uptake of GA allows data acquisition during hepatobiliary phase in addition to dynamic phase examination. In patients with normal liver function, hepatobiliary phase imaging can usually be acquired within 20 min after GA injection. Because of the marked hepatic uptake of GA, this hepatobiliary phase is usually reached within 20 min after initiation of GA in-

jection in patients with normal hepatic function and lasts for at least 60 min (2-7, 9). However, a 20 min wait is too long time consuming on routine liver MR imaging. Liver MR imaging included diffusion-weighted images is available within 15 min. Compared with non-cirrhotic liver, cirrhotic liver may have diminished parenchymal enhancement in the hepatobiliary phase (14). The uptake of GA in cirrhotic liver is variable and may be difficult to predict parenchymal enhancement (14-16).

Although some studies have suggested that decreasing the delay time for the hepatobiliary phase to 10 min sufficient to detect focal hepatic lesions in non-cirrhotic liver (9, 17, 18), there has been no report focused on determining the optimal scan time delay between 10 min, 15 min and 20 min hepatobiliary phase image for the evaluation of small-sized (≤ 3 cm) HCCs in the cirrhotic liver. Therefore, the purpose of this study is to assess the optimal scan delay of the hepatobiliary phase of GA-enhanced MR imaging for small-sized HCCs in the cirrhotic liver.

MATERIALS AND METHODS

Patients

This retrospective study was approved by the review board of our hospital, and followed the guidelines of the Declaration of Helsinki and subsequent amendments. Between Jan. 2009 and Dec. 2010, 182 patients underwent GA-enhanced MR imaging for the evaluation of HCCs in patients with cirrhotic liver. Exclusion criteria included the following: lesions larger than 3 cm or infiltrative lesions ($n = 58$), a history of chemoembolization, ethanol instillation, or thermal ablation within 6 months before study ($n = 70$). Lesions with background hemochromatosis were excluded ($n = 1$) because signal intensity changes of the liver parenchyma due to iron deposition would likely affect measurements for liver to lesion contrast. In final, 53 patients were included in this study.

The patients' age ranged from 40 y to 82 y of age (mean, 60.8 ± 9.9 y). There were 42 male patients and 11 female patients. There were 71 lesions diagnosed as HCCs in 53 patients; 40 patients had solitary lesions, 9 patients had 2 lesions, 3 patients had 3 lesions, and 1 patient had 4 lesions. Among 71 HCCs, 19 were confirmed by surgery, and one was diagnosed by percutaneous biopsy. The remaining HCCs were confirmed by image findings and alpha fetoprotein level > 200 IU/mL in combina-

tion with follow-up imaging obtained more than 6 months later. The criteria for diagnosis of HCCs is as follows (10, 19, 20): 1) a nodule with increased enhancement on arterial phase and wash-out on portal or delayed phase images; 2) a nodule with arterial enhancement and no washout on portal or delayed phase images, but hypointensity on hepatobiliary phases; or 3) a nodule with isointensity during contrast-enhanced dynamic study, hyperintensity on T2-weighted image (T2WI) and no uptake of contrast agent on hepatobiliary phase images.

The mean size of the HCCs was 1.9 cm (range, 0.8-3 cm). There were 11 HCCs equal to or smaller than 1 cm, 33 HCCs were 1-2 cm, and 27 HCCs were larger than 2 cm at maximum diameter. All patients had underlying liver cirrhosis caused by hepatitis B in 39 patients, hepatitis C in 12 patients, alcohol abuse in 6 patients, and idiopathic cirrhosis in 2 patients. Cirrhosis was classified as Child-Pugh class A in 51 patients, as Child-Pugh class B in 1 patient, and Child-Pugh class C in 1 patient (21).

MR Imaging

MR examinations were performed with a 3.0 T MR scanner (Magnetom Tim Trio, Siemens, Munich, Germany) using an 8-channel phased-array coil. The MR imaging protocols was as follows: T1-weighted gradient-echo in-phase imaging [repetition time (TR)/echo time (TE): 4.4 ms/2.5 ms, flip angle: 9.0° , matrix: 320×168 , bandwidth: 680 Hz per pixel]; an out-of-phase imaging (TR/TE: 4.4 ms/1.3 ms, flip angle: 9.0° , matrix: 320×168 , bandwidth: 980 Hz per pixel); a prospective acquisition correction turbo spin echo T2WI (TR/TE: 3000 ms/80 ms, flip angle: 140° , matrix: 320×219 , bandwidth: 260 Hz per pixel), a half-Fourier acquisition single-shot turbo spin-echo heavily T2WI (TR/TE: 1600 ms/182 ms, flip angle: 150° , matrix: 320×230 , bandwidth: 781 Hz per pixel) with a 5-7 mm section thickness, a 1-mm intersection gap, and a field of view of 360×297 mm. A dose of 0.1 mL/kg (0.025 mmol/kg gadoteric acid) contrast agent was bolus injected intravenously at a rate of 1 mL/sec followed by a 20 mL saline solution flush. For contrast-enhanced MR imaging, the unenhanced, dynamic phase (30 s, 60 s, 100 s, 140 s and 180 s after contrast injection) and hepatobiliary phase (10 min, 15 min and 20 min after contrast injection) images were obtained using a fat-suppressed T1-weighted gradient-echo in-phase imaging (TR/TE: 3.4 ms/1.3 ms, flip angle: 13° , matrix: 320×176 , bandwidth: 500 Hz per pixel) with a

3.5 mm section thickness with no intersection gap and a field of view of 360 × 260 mm. Otherwise, T2WIs were obtained between 180 s and 10 minutes; diffusion weighted imaging was obtained between 10 min and 15 min.

Image Analysis

Quantitative Analysis

Quantitative analysis of the reference lesions was performed by one radiologist (J.H.L.) without knowledge of the results of tumor grading on histology. One radiologist calculated signal-to-noise ratio (SNR), enhancement ratio (ER) of the tumor and liver parenchyma and contrast-to-noise ratios (CNR) at 10, 15 and 20 minute images, respectively. Signal intensity (SI) of the liver parenchyma, reference hepatic lesion and background were measured in each patient for all image before and 10, 15 and 20 minutes after contrast injection.

Regions of interest (ROI) were drawn as large as possible in the structure of interest avoiding necrotic areas and vessels. To avoid affection of signal intensity, ROI were drawn on liver parenchyma away from focal hepatic lesions. All ROIs were positioned at identical intra-axial positions for each sequence. Background noise was defined as the standard deviation (SD) of the SI measured in the air outside the body, avoiding artifacts resulting from breathing. SNR, ER of HCCs and liver parenchyma, and liver-to-lesion CNR were calculated with the following formula; $SNR = SI \text{ of liver} / SD \text{ of background noise}$, $ER = [(SI \text{ after enhancement} - SI \text{ before enhancement}) / SI \text{ before enhancement}] \times 100$, and $CNR = [(SI \text{ of tumor} - SI \text{ of liver}) / SD \text{ of background noise}]$.

Qualitative Analysis

Three abdominal radiologists (Y.Y.J, S.S.S, J.W.K) blinded to the results of histology and quantitative analyses reviewed 71 HCCs independently at 10 min, 15 min, and 20 min GA-enhanced hepatobiliary phase MR imaging with additional T1WI, T2WI, heavily T2WI, and dynamic contrast enhanced image. The interval between the reviews of the 3 phases of images was at least 2 weeks. The reference hepatic lesion was evaluated regarding HCC possibility using a 5-point scale: 1, definitely not HCC; 2, probably not HCC; 3, indeterminate; 4, probably HCC; 5, definitely HCC. A score of 0 was assigned retrospectively when an observer did not find a lesion documented as a reference stan-

dard. When an observer estimated the lesion as a score of 4 or 5, the lesion was classified as positive. To achieve accurate correlation between the findings of the scored lesions and the reference standard, each observer recorded the individual image number, the locations of all of the lesions and the diameter of each lesions. For patients with multiple lesions located in the same segment, the observers added further descriptions regarding the size and location of the lesion within each segment in order to avoid confusion during the data analysis.

Statistical Analysis

All statistical analyses were performed with commercially available software (MedCalc for Windows. Version 11.6.1.0; MedCalc Software, Mariakerke, Belgium). For each observer, accuracy [area under the alternative free-response receiver operating characteristic curve (Az)] for the diagnosis of HCCs was calculated and compared by using latent binomial alternative free-response receiver operating characteristic analysis (22, 23). Sensitivity was calculated for the 3 hepatobiliary phases for each observer according to lesion size: equal to or < 1 cm, 1-2 cm, and > 2 cm. Sensitivity was calculated as the number of true-positive lesions divided by the total number of HCCs. For positive predictive value, numbers in parentheses are the number of true-positive lesions divided by the total number of lesions assigned a confidence level of 4 or 5. Statistical analyses for the differences of the sensitivities and positive predictive values (PPV) for each observer were based on a previous report (24).

Descriptive statistics including mean value, standard deviation, and range were calculated for ER, CNR, and SNR. The statistical significance of any differences between calculated ER, CNR, and SNR at 10 min, 15 min, and 20 min was examined using analysis of variance. A *p*-value < 0.05 was considered statistically significant. By comparing the scoring results from the 3 observers with the reference standard, we calculated the kappa value: 0.0-0.2, poor; 0.2-0.4, fair; 0.4-0.6, moderate; 0.6-0.8, good; 0.8-1.0, excellent (25).

RESULTS

Quantitative Analysis

The time course of SNR, ER and CNR between 10, 15 and, 20 minute imaging is shown in Table 1 and Fig. 1. The liver paren-

chyma showed a slight increase in the SNR between 10 and 20 minute imaging. However, significant changes in SNR were not observed. The mean ER of HCCs was maximal at 10 minute imaging. The mean ER of liver parenchyma increased according to time course after GA injection. However, ER of HCCs and liver parenchyma were not statistically significant ($p = 0.569$ and 0.143 , respectively). There were no significant differences in CNR at 10, 15 and 20 minute imaging ($p = 0.279$).

Qualitative Analysis

The calculated Az values for each observer for the GA-enhanced hepatobiliary phase MR imaging are shown in Table 2. The diagnostic accuracy of hepatobiliary phase imaging does not significantly change when performed 10, 15 and 20 minutes after injection (Fig. 2). The average Az values for 10, 15, and 20 minutes between the observers were not significantly different ($p > 0.05$).

The sensitivity and PPV between the 3 hepatobiliary phases

Table 1. Signal-to-Noise Ratio (SNR), Enhancement Ratios (ER) of the Tumor and Liver Parenchyma, and Contrast to Noise Ratio (CNR) on Three Hepatobiliary Phase MR Imaging

Variables	Minutes			p-Value
	10	15	20	
SNR	139.8 ± 55.6	144.5 ± 53.6	146.2 ± 56.8	0.769
ER of tumor	54.2 ± 20.5	49.2 ± 20.0	45.1 ± 24.4	0.119
ER of liver parenchyma	101.7 ± 44.0	109.0 ± 49.5	111.6 ± 51.0	0.569
CNR	-55.5 ± 35.1	-62.8 ± 35.8	-67.1 ± 38.7	0.279

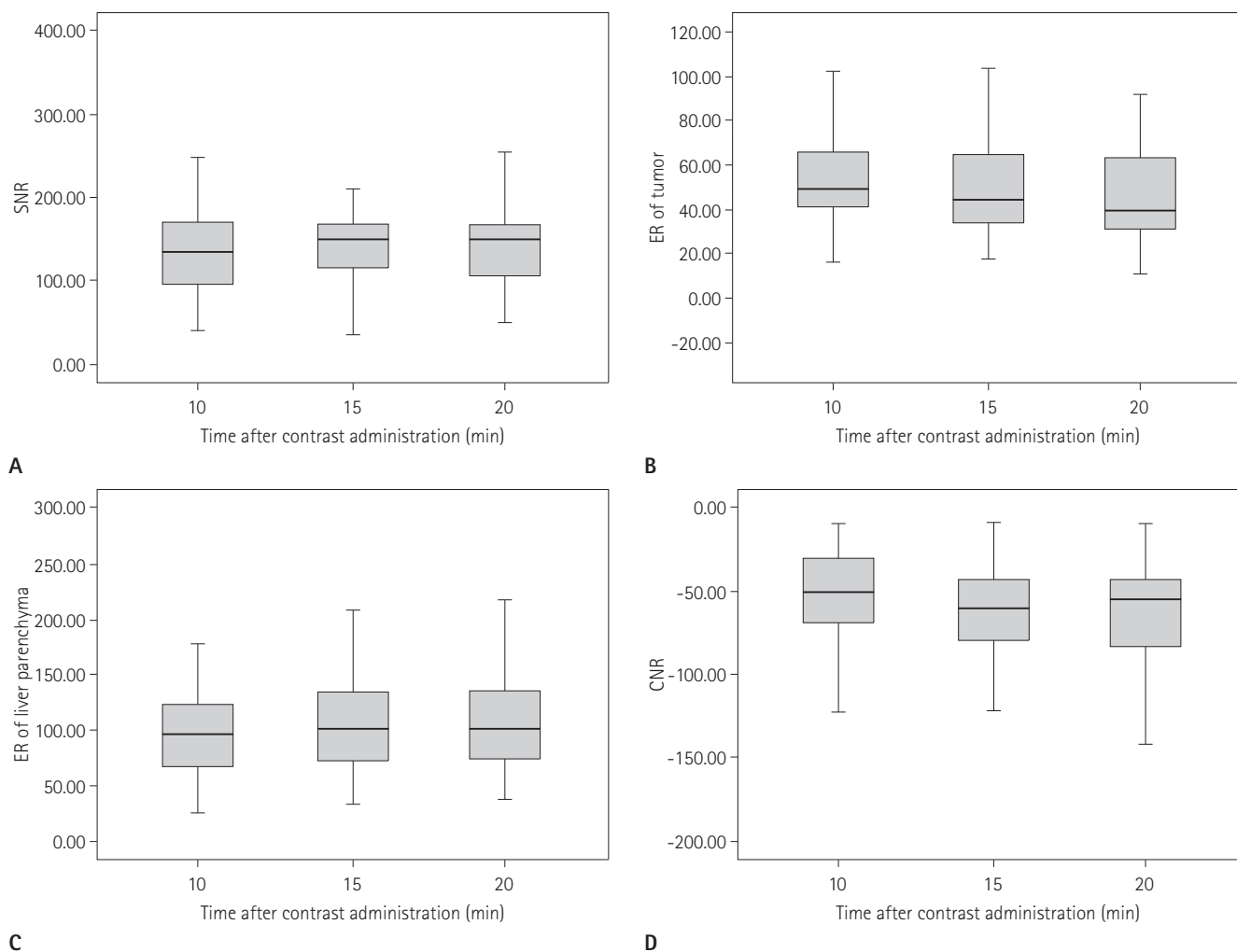


Fig. 1. Signal-to-noise ratios (SNRs) (A), enhancement ratio (ERs) of the tumor (B) and liver parenchyma (C) and contrast-to-noise ratios (CNRs) (D). There are no significant differences in CNR at 10, 15 and 20 minutes imaging after contrast administration.

imaging for each observer are summarized in Table 3. The differences of sensitivity and PPV between the 3 hepatobiliary phase images for each observer were not statistically significant ($p > 0.05$). The PPV of all 3 observers ranged from 81.8% to 86.8%.

The sensitivity and specificity of the 3 observers is shown in Table 4. The sensitivities were increased according to increasing sizes of HCCs. Although 3 observers determined lower sensitivities in the detection of HCCs smaller than 1 cm in diameter,

Table 2. The Az Value for Gadoxetic Acid-Enhanced MR Imaging for the Detection of Hepatocellular Carcinoma by Three Hepatobiliary Phase MR Imaging

Observer	Minutes		
	10	15	20
Observer 1	0.965	0.959	0.950
Observer 2	0.947	0.956	0.967
Observer 3	0.972	0.969	0.965
Average Az value	0.961	0.961	0.960

Table 3. Sensitivity and Positive Predictive Value (PPV) for the Detection of Hepatocellular Carcinoma on Hepatobiliary Phase MR Imaging among Three Observers

Observer	Minutes		
	10	15	20
Sensitivity (%)			
Observer 1	94.3 (67/71)	94.3 (67/71)	90.1 (64/71)
Observer 2	88.7 (63/71)	87.3 (62/71)	91.5 (65/71)
Observer 3	91.5 (65/71)	93.0 (66/71)	93.0 (66/71)
PPV (%)			
Observer 1	83.8 (67/80)	83.8 (67/80)	83.8 (67/80)
Observer 2	81.8 (63/77)	82.7 (62/75)	84.4 (65/77)
Observer 3	83.3 (65/78)	86.8 (66/76)	86.7 (66/77)

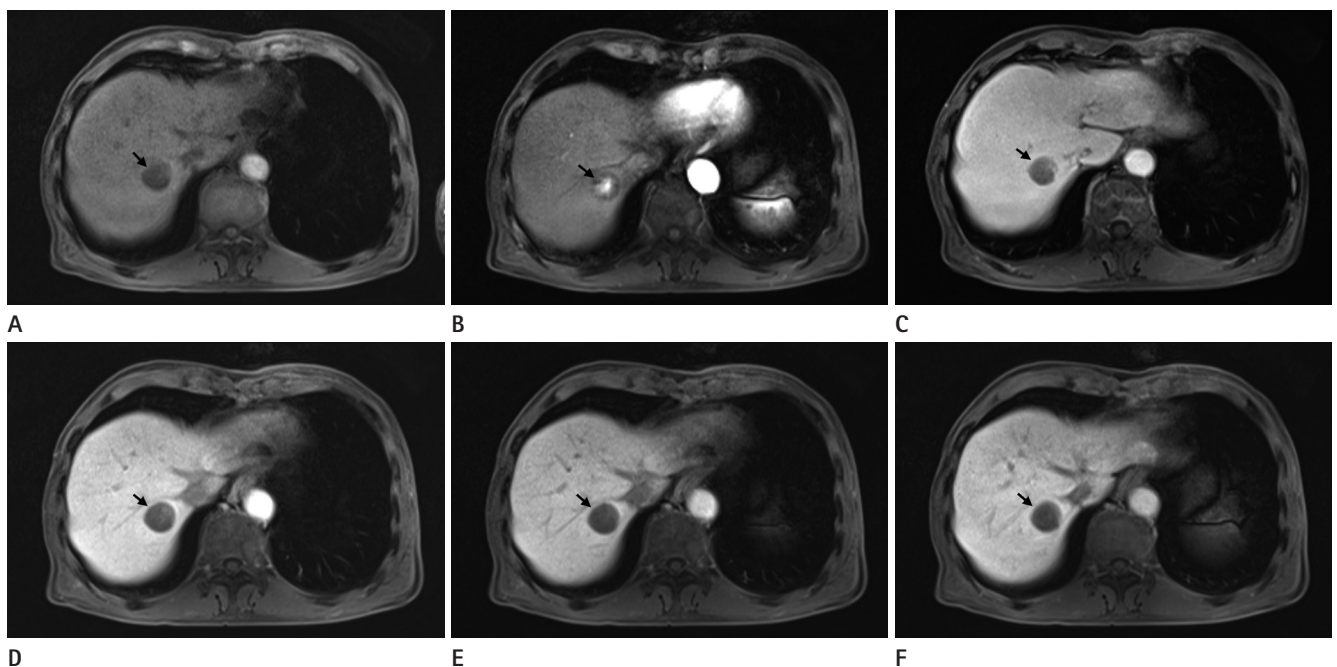


Fig. 2. MR images in 69-year-old man with HCC (arrow) in liver segment VII. Preenhanced image (A), gadoxetic acid-enhanced T1WIs obtained 30 s (B), 180 s (C), 10 minutes (D), 15 minutes (E) and 20 minutes (F) after contrast injection show a 2.1 cm HCC. HCC possibility by all three observers is 5 in the images obtained 10, 15 and 20 minutes after contrast injection. This HCC is confirmed by typical imaging finding on liver MRI (enhancement on arterial phase and washout on portal or delayed phase images).
 Note.—HCC = hepatocellular carcinoma, T1WI = T1 weighted image

the mean sensitivities were similar in all 3 imagings and there was no significant difference was found. The sensitivities for all observers were 100% for all 3 phases of HCCs larger than 2 cm in maximum diameter.

Three observers recorded 22, 17, and 19 false-positive findings on 10 min, 15 min, and 20 min images, respectively. Twelve, 11, and 12 false-positive findings for each observer were most commonly attributed to intrahepatic vasculature. Eight, 5, and 6 false-positive findings for each observer were attributed to cirrhotic nodules.

With regard to the false-negative findings, 24, 22, and 8 lesions were overlooked because of small size below 1 cm, iso-intensity on T2WI, and intrahepatic vasculature on 3 imaging. The one HCC was overlooked by all 3 observers on the 3 imaging, because the liver parenchyma appeared heterogeneous due to the presence of cirrhotic nodules of variable sizes (Fig. 3).

The kappa values among the 3 observers ranged from 0.756 to 0.853, indicating good or excellent agreement for the 3 images.

DISCUSSION

Compared with the non-cirrhotic liver, the cirrhotic liver may have diminished parenchymal enhancement on the hepatobiliary phase after GA injection, and the time to peak enhancement may be delayed. GA enhancement of the cirrhotic liver may be modest and the peak may not be achieved for 40 min or more. The reason for the diminished and delayed enhancement is due to impaired transport mechanism including dysfunctional transporters or reduced functional hepatocytes (26). As in previous studies, our study showed that the liver parenchyma with cir-

rhosis showed a slight increase in the SNR between 10 min and 20 min after GA injection. However, no statistically significant differences in SNR were observed between the 10 min, 15 min, and 20 min MR images.

ER of liver parenchyma was not significantly different between 10 min, 15 min, and 20 min in our study, although it was higher on 20 min images than on 10 min images. Lee et al. (27) also showed that the mean ER of chronic liver disease was not significantly different after 10 min and after 20 min. Reimer et al. (9) showed that CNR was lower on the images obtained 20 min after GA injection than on those obtained after 10 min, but the difference was not significant. Our study showed similar results that there was no significant difference in CNR between 10 min, 15 min, and 20 min images. One of the causes of these consistent results is that most patients in our study had liver cirrhosis that corresponds to a relatively normal liver function. However, according to Frericks et al. (1), CNR decreased significantly between 10 min and 20 min after contrast GA injection. The cause of the inconsistent result is that included HCCs are not limited to small size less than 3 cm and considerable number of Child-Pugh class B was included by Frericks et al.

GA-enhanced MR imaging showed clear superiority in the detection of HCCs in cirrhotic liver. The sensitivities of GA-enhanced MR imaging for detection of HCCs ranged from 81.3 to 99.4% in previous studies (10, 28-32). The hepatobiliary phase MR imaging may be useful in detecting iso- and hypovascular small HCCs that are nonspecific in the dynamic phases (16). Haradome et al. (28) demonstrated that the sensitivity of hepatobiliary phase MR imaging for detection of early stage HCCs (range 0.5-2.8 cm, mean size 1.7 cm) was 93.0%. In our study,

Table 4. Comparison of the Sensitivities and Specificities between 10, 15 and 20 Minutes Hepatobiliary Phase MR Imaging According to Lesion Size by Three Radiologists

Lesion Size	Minutes		
	10	15	20
Sensitivity (%)			
< 1.0 cm	69.7 (23/33)	69.7 (23/33)	78.8 (26/33)
1.0-2.0 cm	92.9 (92/99)	93.9 (93/99)	90.9 (90/99)
> 2.0 cm	100 (81/81)	100 (81/81)	100 (81/81)
Mean	92.0 (196/213)	92.4 (197/213)	92.4 (197/213)
Specificity (%)			
< 1.0 cm	98.9 (1225/1239)	99.1 (1229/1239)	99.1 (1229/1239)
1.0-2.0 cm	99.7 (1169/1173)	99.4 (1167/1173)	99.7 (1169/1173)
> 2.0 cm	99.8 (1189/1191)	99.8 (1189/1191)	99.7 (1188/1191)
Mean	99.5 (3583/3603)	99.6 (3585/3603)	99.6 (3586/3603)

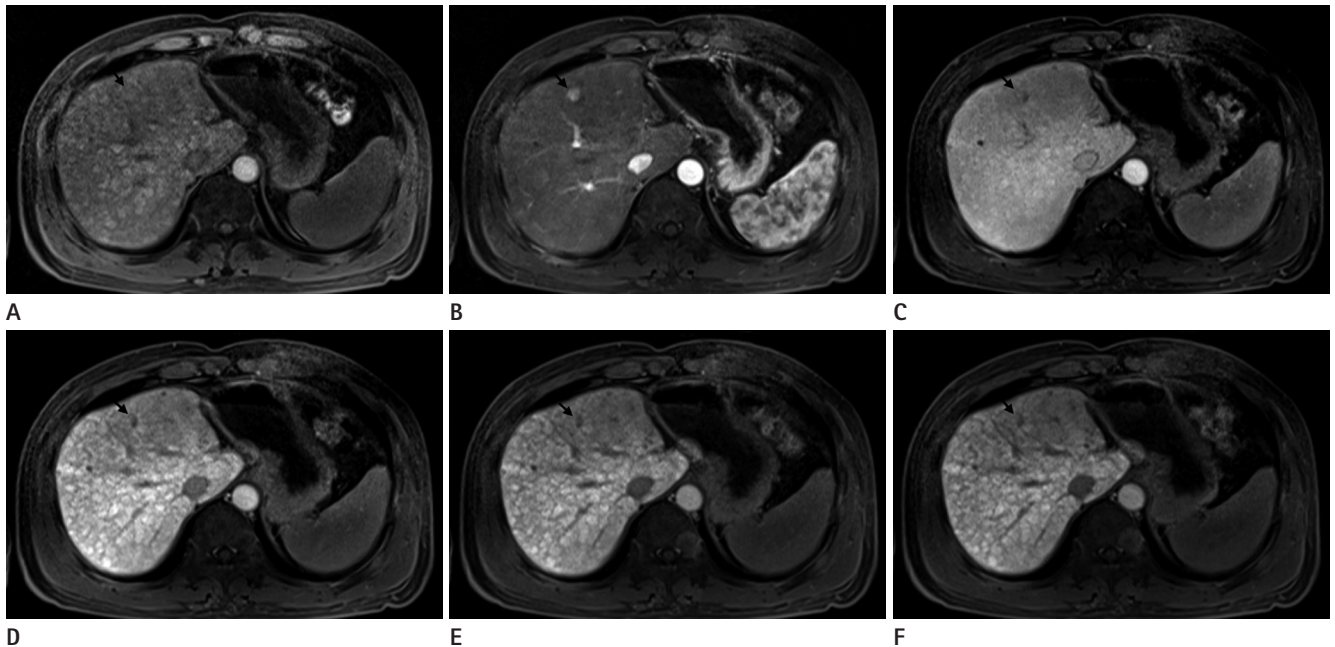


Fig. 3. MR images in 57-year-old man with HCC (arrow) in liver segment IV. Preenhanced image (A), gadoteric acid-enhanced T1WIs obtained 30 s (B), 180 s (C), 10 minutes (D), 15 minutes (E) and 20 minutes (F) after contrast injection show a 1 cm HCC. This HCC is overlooked by all three observers because of multiple cirrhotic nodules of variable sizes. This HCC is confirmed by typical imaging finding on liver MRI (enhancement on arterial phase and washout on portal or delayed phase images). Note.—HCC = hepatocellular carcinomas, T1WI = T1 weighted image

the sensitivities of hepatobiliary phase MR imaging for detecting HCCs smaller than 3 cm were 92.0, 92.4 and 92.4% at 10 min, 15 min, and 20 min, respectively. Our result was consistent with previous reports because of the same contrast medium and the small HCC size in cirrhotic liver chosen.

However, pre-enhanced and dynamic phase images may lead to an increased in detection of HCC. Small HCCs showing typical arterial enhancement and washout on portal or delayed phase images were seen as isointense or slightly hypointense lesions on hepatobiliary phase image. The reason of decreased detection of HCC may be related to residual hepatocyte activity due to well-differentiated lesion and heterogeneous hepatic parenchyma due to the presence of cirrhotic nodules.

In our study, the numbers of false-positive lesions by 3 observers were similar between 10 min, 15 min, and 20 min images. The false-positive lesions were caused by intrahepatic vasculature and cirrhotic nodules. The liver parenchyma of cirrhotic liver appeared heterogeneous due to the presence of cirrhotic nodules of variable sizes and signal intensity interdispersed in a mesh of hypointense fibrotic scars that may be fine, coarse, nodular or confluent (32). Previous reports (28, 30) showed that the false-positive findings for detection of HCCs on GA-enhanced

MR imaging were attributed to arterio-portal (AP) shunts and high-flow hemangioma. AP shunts usually exhibit intense enhancement on arterial phase images and identical signal intensity to that of surrounding liver parenchyma on GA-enhanced equilibrium or hepatobiliary phase MR imaging. The presence of high signal intensity on T2WI for hemangioma could be helpful for differentiating high-flow hemangiomas from HCC. AP shunts and hemangioma could not be false-positive findings because the assessment in our study included moderate, heavily T2WI and hepatobiliary phase MR imaging.

The numbers of false-negative lesions by three observers were same between the 10, 15 and 20 minutes images. Fifty-four HCCs, which were interpreted as a false-negative lesions from the 3 phases for each observer were too small to be interpreted as such according to the diagnostic criteria, were isointense to the surrounding parenchyma on T2WI, or overlooked because of intravascular structures. Small HCCs may not show definite hypointensity on hepatobiliary phase MR imaging due to retention of GA in well-differentiated HCC and/or decreased parenchymal enhancement in the cirrhotic background liver (32). According to the diagnostic criteria of our study, since small HCCs did not show a definite hypointensity on hepatobiliary phase

MR imaging, it was not regarded as HCC.

Our study has several limitations: first, only 20 HCCs were pathologically confirmed, the rest of the reference tumors were diagnosed by imaging and clinical data. The inclusion of only those lesions that were confirmed at pathologic examination could have led to a verification bias. Second, this study included 51 patients with cirrhosis of Child-Pugh class A, which corresponded to liver cirrhosis. It was possible that they had relatively normal liver function. The number of patients with Child-Pugh class B or C, which could lead to an increased false negative rate, was too small to compare the other 2 classes. We could not compare quantitative and qualitative evaluation of the reference tumors according to liver function in the hepatobiliary phase MR imaging. Further studies should be performed to compare differences of qualitative and quantitative evaluation between Child-Pugh classes of A, B and C.

In conclusion, hepatobiliary phase MR imaging obtained 10 min, 15 min, and 20 min yield comparable diagnostic information, so that the choice of scan delay can be adapted according to the clinical routine needs to evaluate small-sized HCCs in cirrhotic liver.

REFERENCES

- Frericks BB, Loddenkemper C, Huppertz A, Valdeig S, Stroux A, Seja M, et al. Qualitative and quantitative evaluation of hepatocellular carcinoma and cirrhotic liver enhancement using Gd-EOB-DTPA. *AJR Am J Roentgenol* 2009;193:1053-1060
- Ringe KI, Husarik DB, Sirlin CB, Merkle EM. Gadoteric acid-enhanced MRI of the liver: part 1, protocol optimization and lesion appearance in the noncirrhotic liver. *AJR Am J Roentgenol* 2010;195:13-28
- Hamm B, Staks T, Mühler A, Bollow M, Taupitz M, Frenzel T, et al. Phase I clinical evaluation of Gd-EOB-DTPA as a hepatobiliary MR contrast agent: safety, pharmacokinetics, and MR imaging. *Radiology* 1995;195:785-792
- Reimer P, Rummeny EJ, Shamsi K, Balzer T, Daldrup HE, Tombach B, et al. Phase II clinical evaluation of Gd-EOB-DTPA: dose, safety aspects, and pulse sequence. *Radiology* 1996;199:177-183
- Vogl TJ, Kümmel S, Hammerstingl R, Schellenbeck M, Schumacher G, Balzer T, et al. Liver tumors: comparison of MR imaging with Gd-EOB-DTPA and Gd-DTPA. *Radiology* 1996;200:59-67
- Saito K, Kotake F, Ito N, Ozuki T, Mikami R, Abe K, et al. Gd-EOB-DTPA enhanced MRI for hepatocellular carcinoma: quantitative evaluation of tumor enhancement in hepatobiliary phase. *Magn Reson Med Sci* 2005;4:1-9
- Hammerstingl R, Huppertz A, Breuer J, Balzer T, Blakeborough A, Carter R, et al. Diagnostic efficacy of gadoteric acid (Primovist)-enhanced MRI and spiral CT for a therapeutic strategy: comparison with intraoperative and histopathologic findings in focal liver lesions. *Eur Radiol* 2008;18:457-467
- Lee JM, Zech CJ, Bolondi L, Jonas E, Kim MJ, Matsui O, et al. Consensus report of the 4th International Forum for Gadolinium-Ethoxybenzyl-Diethylenetriamine Pentaacetic Acid Magnetic Resonance Imaging. *Korean J Radiol* 2011;12:403-415
- Reimer P, Rummeny EJ, Daldrup HE, Hesse T, Balzer T, Tombach B, et al. Enhancement characteristics of liver metastases, hepatocellular carcinomas, and hemangiomas with Gd-EOB-DTPA: preliminary results with dynamic MR imaging. *Eur Radiol* 1997;7:275-280
- Ahn SS, Kim MJ, Lim JS, Hong HS, Chung YE, Choi JY. Added value of gadoteric acid-enhanced hepatobiliary phase MR imaging in the diagnosis of hepatocellular carcinoma. *Radiology* 2010;255:459-466
- Chou CT, Chen YL, Su WW, Wu HK, Chen RC. Characterization of cirrhotic nodules with gadoteric acid-enhanced magnetic resonance imaging: the efficacy of hepatocyte-phase imaging. *J Magn Reson Imaging* 2010;32:895-902
- Sano K, Ichikawa T, Motosugi U, Sou H, Muhi AM, Matsuuda M, et al. Imaging study of early hepatocellular carcinoma: usefulness of gadoteric acid-enhanced MR imaging. *Radiology* 2011;261:834-844
- Goodwin MD, Dobson JE, Sirlin CB, Lim BG, Stella DL. Diagnostic challenges and pitfalls in MR imaging with hepatocyte-specific contrast agents. *Radiographics* 2011;31:1547-1568
- Cruite I, Schroeder M, Merkle EM, Sirlin CB. Gadoteric acid-enhanced MRI of the liver: part 2, protocol optimization and lesion appearance in the cirrhotic liver. *AJR*

- Am J Roentgenol* 2010;195:29-41
15. Nilsson H, Nordell A, Vargas R, Douglas L, Jonas E, Blomqvist L. Assessment of hepatic extraction fraction and input relative blood flow using dynamic hepatocyte-specific contrast-enhanced MRI. *J Magn Reson Imaging* 2009;29:1323-1331
 16. Ryeom HK, Kim SH, Kim JY, Kim HJ, Lee JM, Chang YM, et al. Quantitative evaluation of liver function with MRI Using Gd-EOB-DTPA. *Korean J Radiol* 2004;5:231-239
 17. Motosugi U, Ichikawa T, Tominaga L, Sou H, Sano K, Ichikawa S, et al. Delay before the hepatocyte phase of Gd-EOB-DTPA-enhanced MR imaging: is it possible to shorten the examination time? *Eur Radiol* 2009;19:2623-2629
 18. Zech CJ, Grazioli L, Breuer J, Reiser MF, Schoenberg SO. Diagnostic performance and description of morphological features of focal nodular hyperplasia in Gd-EOB-DTPA-enhanced liver magnetic resonance imaging: results of a multicenter trial. *Invest Radiol* 2008;43:504-511
 19. Willatt JM, Hussain HK, Adusumilli S, Marrero JA. MR Imaging of hepatocellular carcinoma in the cirrhotic liver: challenges and controversies. *Radiology* 2008;247:311-330
 20. Kudo M, Han KH, Kokudo N, Cheng AL, Choi BI, Furuse J, et al. Liver Cancer Working Group report. *Jpn J Clin Oncol* 2010;40 Suppl 1:i19-i27
 21. Pugh RN, Murray-Lyon IM, Dawson JL, Pietroni MC, Williams R. Transection of the oesophagus for bleeding oesophageal varices. *Br J Surg* 1973;60:646-649
 22. Chakraborty DP, Winter LH. Free-response methodology: alternate analysis and a new observer-performance experiment. *Radiology* 1990;174(3 Pt 1):873-881
 23. Hanley JA, McNeil BJ. A method of comparing the areas under receiver operating characteristic curves derived from the same cases. *Radiology* 1983;148:839-843
 24. Bennett BM. On comparisons of sensitivity, specificity and predictive value of a number of diagnostic procedures. *Biometrics* 1972;28:793-800
 25. Fleiss JL, Levin B, Paik MC. *The measurement of interrater agreement. Statistical methods for rates and proportions, 2nd ed.* New York: John Wiley & Sons, 1981:212-236
 26. Tajima T, Takao H, Akai H, Kiryu S, Imamura H, Watanabe Y, et al. Relationship between liver function and liver signal intensity in hepatobiliary phase of gadolinium ethoxybenzyl diethylenetriamine pentaacetic acid-enhanced magnetic resonance imaging. *J Comput Assist Tomogr* 2010;34:362-366
 27. Lee WJ, Cha SH, Kim MY, Chung HH, Lee SW, Yi A, et al. Quantitative evaluation of the hepatic parenchymal change in patients with chronic liver disease using Gd-EOB-DTPA-enhanced MRI: comparison with normal liver. *J Korean Soc Radiol* 2011;64:49-55
 28. Haradome H, Grazioli L, Tinti R, Morone M, Motosugi U, Sano K, et al. Additional value of gadoxetic acid-DTPA-enhanced hepatobiliary phase MR imaging in the diagnosis of early-stage hepatocellular carcinoma: comparison with dynamic triple-phase multidetector CT imaging. *J Magn Reson Imaging* 2011;34:69-78
 29. Park Y, Kim SH, Kim SH, Jeon YH, Lee J, Kim MJ, et al. Gadoteric acid (Gd-EOB-DTPA)-enhanced MRI versus gadobenate dimeglumine (Gd-BOPTA)-enhanced MRI for preoperatively detecting hepatocellular carcinoma: an initial experience. *Korean J Radiol* 2010;11:433-440
 30. Kim SH, Kim SH, Lee J, Kim MJ, Jeon YH, Park Y, et al. Gadoteric acid-enhanced MRI versus triple-phase MDCT for the preoperative detection of hepatocellular carcinoma. *AJR Am J Roentgenol* 2009;192:1675-1681
 31. Kim YK, Kim CS, Han YM, Kwak HS, Jin GY, Hwang SB, et al. Detection of hepatocellular carcinoma: gadoteric acid-enhanced 3-dimensional magnetic resonance imaging versus multi-detector row computed tomography. *J Comput Assist Tomogr* 2009;33:844-850
 32. Golfieri R, Renzulli M, Lucidi V, Corcioni B, Trevisani F, Bolondi L. Contribution of the hepatobiliary phase of Gd-EOB-DTPA-enhanced MRI to Dynamic MRI in the detection of hypovascular small (≤ 2 cm) HCC in cirrhosis. *Eur Radiol* 2011;21:1233-1242

간경변증 환자에서 소간세포암평가를 위한 Gadoteric Acid 조영증강 자기공명영상의 적절한 스캔지연¹

이지현² · 정용연¹ · 허숙희¹ · 신상수² · 김진웅¹ · 강형근¹

목적: 간경변증 환자에서 3 cm 이하의 소간세포암평가를 위한 gadoteric acid 조영증강 자기공명영상의 hepatobiliary phase의 적절한 스캔지연에 대하여 평가하였다.

대상과 방법: Gadoteric acid 조영증강 자기공명영상 hepatobiliary phase를 시행한 53명의 간경변증 환자가 포함되었다. Hepatobiliary phase 영상은 조영제 주입 후 10, 15, 20분 후에 얻었다. 정량분석으로 신호대잡음비(signal-to-noise ratio), 간세포암과 간실질의 조영증강비(enhancement ratio), 대조잡음비(contrast-to-noise)를 측정하였다. 정성분석을 위해 세 명의 영상의가 10, 15, 20분 영상에서 병소뚜렷함을 측정하였으며 진단 정확도를 위해 Az를 비교하였다. 민감도와 특이도를 측정하였다.

결과: 10, 15, 20분 자기공명영상에서 신호대잡음비, 간세포암과 간실질의 조영증강비, 대조잡음비는 뚜렷한 차이를 보이지 않았다($p = 0.769, 0.119, 0.569$ and 0.279). Lesion possibility의 Az value는 10, 15, 20분 영상에서 의미있는 차이를 보이지 않았다($Az = 0.961, 0.961$ and 0.960). 민감도와 특이도에서도 뚜렷한 차이를 보이지 않았다($p > 0.05$).

결론: 간경변증 환자에서 3 cm 이하의 소간세포암평가를 위한 gadoteric acid 조영증강 자기공명영상 10, 15분 영상은 20분 영상과 큰 차이 없으며, 10, 15분 영상이 20분 지연 없이 대체할 수 있다.

¹전남대학교 의과대학 화순전남대학교병원 영상의학과, ²전남대학교 의과대학 전남대학교병원 영상의학과